Journal of Applied Polymer Science

Solvent-free synthesis of chiral molecularly imprinted polymers: Porosity control using a nano-sized solid porogen

Mariana Duarte,[1,2] Johan Billing,[1] Ecevit Yilmaz[1]

[1]MIP Technologies AB, A Subsidiary of Biotage AB, Box 737, Lund, 22007, Sweden

[2]Department of Biomedical Engineering, Division of Nanobiotechnology, Lund University, Box 118, Lund, 22100, Sweden

Correspondence to: M. Duarte (E-mail: mariana.duarte@bme.lth.se)

ABSTRACT: Molecularly imprinted polymers (MIPs) have been synthesized in the absence of a solvent using fumed silica nanoparticles to create a porous network. The method employed led to a chiral imprinting effect and allowed for an excellent control over the internal morphology of imprinted and non-imprinted polymer (NIP) materials. The polymers possess high surface areas (>300 m^2) and identical pore size (112 Å). The MIP exhibited an imprinting factor (IF) of 9 and a selectivity value (α) of 1.83 for (−)-ephedrine. © 2016 Wiley Periodicals, Inc. J. Appl. Polym. Sci. **2016**, *133*, 44104.

KEYWORDS: molecular recognition; morphology; nanoparticles; porous materials

Received 29 February 2016; accepted 9 June 2016

DOI: 10.1002/app.44104

INTRODUCTION

Molecular imprinting is a technique that imparts selectivity toward a target molecule to a material. In this technique, a polymeric material is formed in the presence of a template molecule and can be used as a selective adsorbent or in a sensor.[1,2] Molecularly imprinted polymers (MIPs) have traditionally been synthesized in a monolithic form using a mixture of monomers and a solvent to confer porosity to the polymer. Additionally, several synthesis techniques have been developed over the years and new formats of MIPs have been produced by suspension and precipitation polymerization as well as by grafting and hard templating methods using silica beads;[3–11] these techniques bring advantages related to particle shape and size, binding site accessibility, facile mass transfer, easier and faster preparation, avoidance of grinding and sieving, etc. However, despite these developments, MIPs are still most commonly synthesized with liquid solvents which are added as porogens to impart porosity and to dissolve the pre-polymerization mixture. This is a crucial parameter as these solvents can interfere with the interaction between template and functional monomer, thus weakening or even completely eliminating the imprinting effect on the polymer. Hence, solvent optimization is an unavoidable and important step in traditional MIP synthesis protocols.

When used for adsorption, surface areas in the hundreds of square meters per gram are generally most desirable, which is difficult to achieve by templating methods alone. Furthermore, it is possible to tailor the porosity in the micro, meso, and macro ranges by tuning the composition of the porogen, which can be composed of one single solvent or a combination of different ones. In general, the Hansen solubility parameters can give a good indication of the effect on the porosity;[12] solvents and monomers with similar solubility parameters will interact more and thus create more micropores. For all the reasons stated above, liquid porogens are the first choice in polymer synthesis.[4,13,14]

Nonetheless, in the case of MIPs, a liquid porogen imposes an increased risk that the solvent may disrupt the template–monomer interactions, leading to the need for extensive practical or theoretical optimization strategies.[15,16] In conclusion, a good pore forming, high surface area generating solvent could compete with the imprinting complex and thus be of little practical use or even detrimental to create highly selective MIPs.[17] Moreover, the evaluation of the imprinting effect is also dependent on the surface areas of the MIP and the NIP, but obtaining an identical morphological structure in both polymers is not a straightforward task when using liquid porogens as the template can affect the solubility parameters. In these cases, the assessment of selectivity and imprinting factors can be misleading, as a stronger retention of the target molecule might be instead due to surface area discrepancies. Assuring an identical surface area in the MIP and NIP materials can therefore facilitate the evaluation of these parameters.

In a previous study we have concluded that fumed silica can function as a solid porogen in cross-linked polymers synthesis.[18]

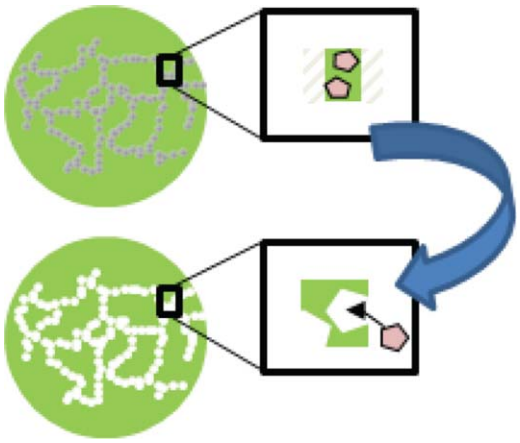

Scheme 1. Dispersed fumed silica nanoparticles as solid porogen in the synthesis of a molecularly imprinted polymer (MIP). The aggregation of the nanoparticles creates a pore-forming network (gray), which, after etching, leaves voids (white) which constitute the pores with accessible binding sites for the target molecule (pink pentagons). [Color figure can be viewed in the online issue, which is available at wileyonlinelibrary.com.]

The non-imprinted poly(divinylbenzene) materials were mesoporous materials with high surface areas and the silica particle size was replicated in the polymer average pore size. In this work, we have included methacrylic acid as a functional monomer and ephedrine as a model template, to provide a proof of concept of the applicability of this method to molecularly imprinted polymers (Scheme 1). Ephedrine has been used extensively in MIP synthesis[19–22] and chiral separation has been reported when using sacrificial supports.[9,23]

EXPERIMENTAL

Divinylbenzene (DVB) 80% grade (previously treated with aluminum oxide to remove the stabilizer), methacrylic acid (MAA), (−)-ephedrine, (+)-ephedrine hydrochloride, 2,2'-azobis(2,4-dimethylvaleronitrile) (ABDV), and HPLC-grade solvents were purchased from Sigma-Aldrich (Steinheim, Germany). Fumed silica nanoparticles (Aerosil R8200) were obtained from Evonik (Essen, Germany). Distilled water was purified using an ultrapure water system from Elga (High Wycombe, The United kingdom). In 500 mL glass bottles, (−)-ephedrine (10 g, 0.06052 mol), MAA (20.83 g, 0.2421 mol), DVB (157.59 g, 1.210 mol), and ABDV (1.784 g) were dissolved. To this solution, 110 g of fumed silica was slowly added and the mixture was gently stirred with a spatula to obtain a thick paste. The mixture was then purged with N_2 and placed in an oven at 60 °C for approximately 16 h. After polymerization, the resulting monolith was crushed in a mortar and the particles were sieved between 20 and 32 μm. Porous polymer particles were obtained after removal of the silica with 3*M* NaOH in 40% MeOH in water. 20 mL of NaOH solution was used per gram of silica. The mixture was sonicated and then stirred for 3 days (at room temperature). After completion of the silica removal step, the polymer particles were washed with abundant warm water several times and finally twice with methanol before being subjected to a Soxhlet extraction to ensure total removal of the template using MeOH/1*M* HCl (80:20 v/v) for 24 h. A final wash with acetone was done before the polymers were left to dry in a vacuum oven at 40 °C overnight. NIP particles were obtained in a similar way, without the use of the template. To confirm the removal of the silica and the template, elemental analyses were performed at Mikroanalytisches Labor Kolbe (Mülheim, Germany). Pore volumes and surface areas were obtained by N_2 adsorption analyses which were run on a Micromeritics ASAP 2400 at the Department of Chemical Engineering, Chemical Centre, Lund University. Transmission electron microscopy (TEM) images were obtained at the Department of Biology, Lund University. The samples were embedded in Agar 100 EPON using acetone and sectioned on a Leica UC7 ultra-microtome. 50 nm sections were mounted on Pioloform® coated copper grids and imaged at 80 kV with a JEOL 1400 plus.

MIP and NIP particles (20 − 32 μm) were packed in HPLC columns of 4.6 mm i.d. × 150 mm by a high-pressure down-fill column slurry packing procedure, using water and an air-driven pump. The chromatography evaluation experiments were run using a Shimadzu LC-10AD equipped with a UV detector. In order to prepare its free base, (+)-ephedrine hydrochloride (2.02 g, 10 mmol) was dissolved in water and poured into a separation funnel. A solution of sodium hydroxide in water (120 mL, 0.1*M*) was added and the mixture was extracted three times with dichloromethane (100 mL). The combined extracts were dried over sodium sulfate and concentrated to obtain (+)-ephedrine free base. Solutions of 1 g/L of (+)-ephedrine and (−)-ephedrine were prepared in water. HPLC experiments were carried out in isocratic mode with 95% MeOH and 5% 100 m*M* ammonium acetate buffer (pH 3.6). The flow rate was 1 mL/min and the sample injection volume was 5 μL.

RESULTS AND DISCUSSION

MIP particles were prepared using a template:functional monomer:cross-linker molar ratio of 1:4:20 and fumed silica of an average primary particle size of 12 nm as solid porogen. Porous polymer particles were obtained after dissolution of the silica using sodium hydroxide.

The polymers were tested in FT-IR to confirm the effective removal of the silica particles (Figure 1) which is indicated by

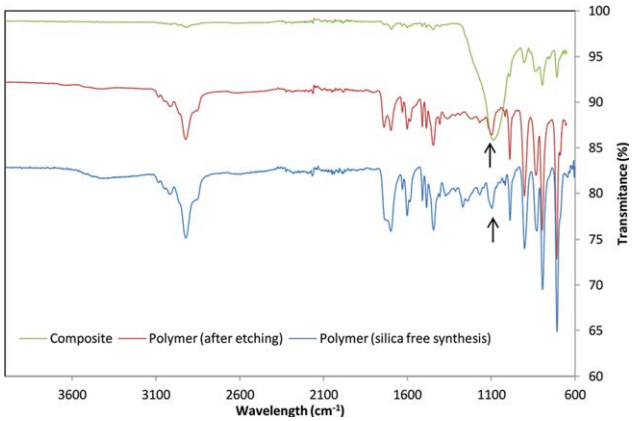

Figure 1. FT-IR spectra of the silica-MIP composite (green line), the MIP after the etching of the silica (red line) and a reference polymer synthetized in the absence of silica (blue line). [Color figure can be viewed in the online issue, which is available at wileyonlinelibrary.com.]

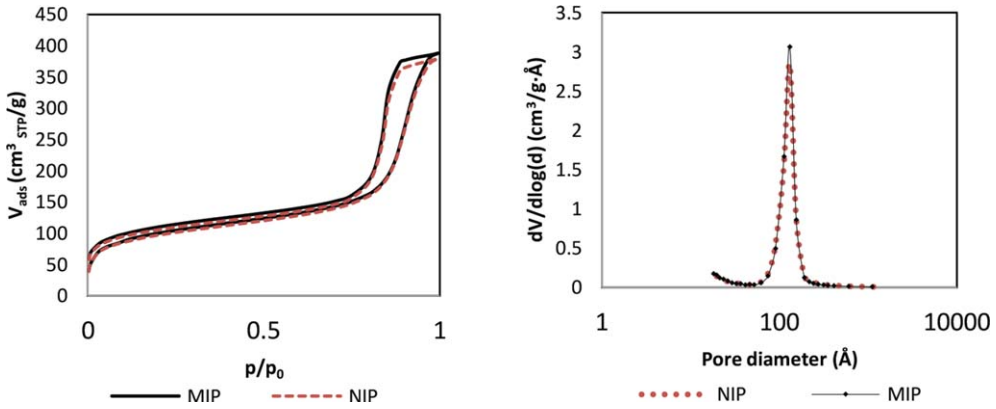

Figure 2. (a) (left) Isotherms obtained by nitrogen adsorption on the MIP and the NIP. (b) (right) Pore size distribution calculated with the BJH method from the desorption branch of the isotherm of the MIP and of the NIP. [Color figure can be viewed in the online issue, which is available at wileyonlinelibrary.com.]

the absence of the siloxane bond—a band at approximately 1080 cm^{-1}—and the spectrum of the MIP after removal of silica is identical to that of a polymer with the same composition synthesized in the absence of silica.

Additionally, elemental analyses were performed to support the spectroscopy data and the results showed Si residues of 0.53% Si in the MIP and 0.86% Si in the NIP. The initial theoretical Si content is 17.7% as calculated from the synthesis protocol and therefore, this analysis confirmed that over 95% of the silica is successfully removed from the polymers after etching.

The polymers were expected to have similar pore size distributions which was confirmed by the pore analyses obtained by nitrogen adsorption according to the BET method.[24] The isotherms and pore size distributions of both polymers are shown in Figure 2(a,b), respectively. Figure 2(b) shows the similarity of the pore size and the pore volume (area under the curve) of both polymers and the curves overlap to a large extent. The values are also presented in Table I. Similarly, the adsorption and desorption isotherms [Figure 2(a)] characterize polymers with very similar pore structure with pores in the mesoporosity range, as indicated by the hysteresis loop and in conformity with the pore size distribution. The mean pore size in both polymers confirms that the silica particle size was replicated in the pores of the polymer. Additionally, the polymers exhibit high surface areas (>300 m^2/g) which enable the use in applications such as adsorption and chromatography.

The use of fumed silica particles to template the pore network on the polymer is dependent on their surface characteristics. The compatibility of a very hydrophobic cross-linker, such as the divinylbenzene used in this synthesis, with hydrophobic surface modified fumed silica allows for the incorporation of a sufficient volume of silica particles in the pre-polymerization mixture which results in reasonably high pore volumes (>0.5 mL/g). However, we have previously studied this parameter using a composition of divinylbenzene without any other co-monomers and were able to obtain a larger pore volume, which is due to a higher percolation threshold.[18] Hence, the presence of more hydrophilic monomers may require an assessment of the possible surface modifications on the silica. Nonetheless, the nitrogen adsorption study confirmed that the consistency of pore size is maintained even when methacrylic acid is used. This finding highlights the robustness of the method and, additionally, its capability for porosity control in molecularly imprinted polymers, since the pore creation mechanism is not greatly influenced by the presence of the template, as opposed to liquid porogens.

TEM micrographs at two different magnifications are shown in Figure 3. The polymer is represented by the dark shaded areas and the pores by the light shaded areas. These images complement the BET data showing that these polymers have a porous structure that is well connected.

The evaluation of the imprinting effect was performed via the chromatographic method. The resulting MIPs and NIPs were tested in packed columns, using single analyte injections of both ephedrine enantiomers. The retention times can be found in Table II and the elution profiles of the ephedrine enantiomers on both polymers are shown in Figure 4.

The selectivity and the imprinting factor of the MIP and NIP were calculated according to eqs. (1) and (2):

$$\alpha = \frac{t_{r,\ (-)E} - t_{r,\ void}}{t_{r,\ (+)E} - t_{r,\ void}} \quad (1)$$

$$IF = \frac{t_{r,\ (-)E_{MIP}} - t_{r,\ void}}{t_{r,\ (-)E_{NIP}} - t_{r,\ void}} \quad (2)$$

where t_r is the retention time of the analyte $(-)E$ or $(+)E$ in the MIP or in the NIP column.

$t_{r,\ void}$ was measured by injecting 5 µL of 1 g/L of sodium nitrite in water.

Table I. Pore Morphology Values Obtained by BET

	Pore size (Å)	Surface area (m^2/g)	Pore volume (mL/g)
MIP	112	358	0.60
NIP	112	343	0.59

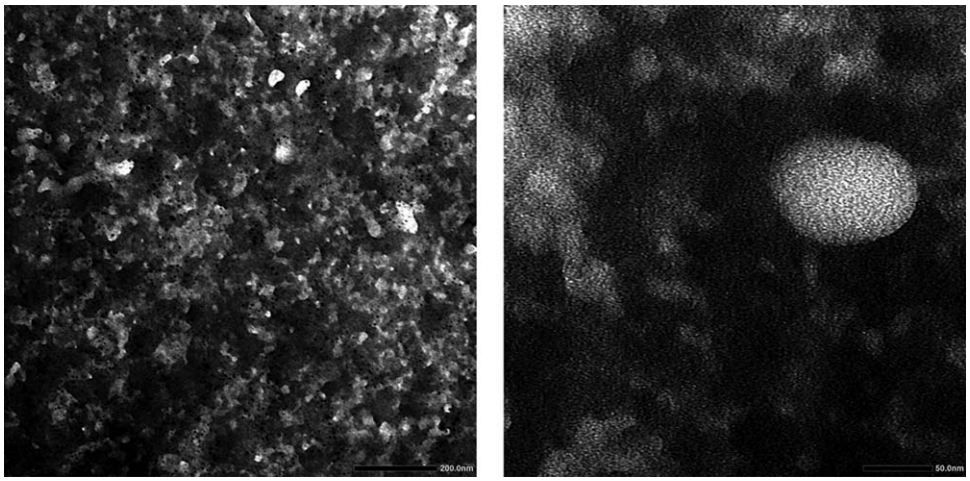

Figure 3. TEM images showing the internal porosity of the MIP.

The selectivity (α) values found were calculated by eq. (1) using the retention time values present in Table II and are 1.83 for the MIP and close to 1 for the NIP. The imprinting factor calculated by eq. (2) was 9. The fact that both polymers are identical in their physical-chemical properties, which is the main aim of the use of a solid porogen, alongside with a full control over the pore size (by replication of the silica particle size), constitutes a strong basis to assure that the selectivity of the MIP is due to the creation of cavity-like binding sites by the imprinting technique. Thus, these results clearly show the successful imprinting of (−)-ephedrine with the presented method.

In Figure 4 it is observable that, as expected, the non-imprinted material does not provide discrimination between the enantiomers nor does it retain significantly any of them under the chromatography conditions used. The MIP however, provides higher retention of both enantiomers with selectivity toward the template (−)-ephedrine which has a longer retention time; in addition to a higher retention time, a peak "tailing" shape, characteristic of MIP adsorption,[25] is visible.

CONCLUSIONS

We demonstrate here for the first time the applicability of fumed silica as a pore forming agent in a system of MIPs. The pore structures of the polymers were obtained by the use of a versatile solid nanoparticle porogen which imparts a series of advantages for MIP design and synthesis. Those may include a large applicability to a broad spectrum of monomer systems, consistency and uniformity in pore size distribution and high batch reproducibility independent of the presence of the template resulting in MIPs and NIPs with essentially equal porosity. Even if (−)-ephedrine MIPs have been synthesized using several methods before,[26–30] the fact that the creation of accessible chiral sites was accomplished without the use of a liquid porogen while guaranteeing the replication of the pore morphology in the NIP is, to the best of our knowledge, unique in molecular imprinting technology. Additionally, and perhaps most importantly, the work described in this article decouples the porogenic and solvation capabilities of the liquid solvents, which have been the main approach to MIP synthesis until present date. This approach opens up interesting new possibilities of employing assisting liquid monomers to help dissolving the monomer–template complex. We expect that the use of solid porogens that can be removed after polymerization opens up possibilities for MIP formulations that may vastly strengthen the imprinting effect. In addition, due to the excellent control over the porosity of the polymers, this constitutes an innovative and important finding in the field of molecular imprinting as the direct comparison of binding properties is better facilitated when morphology effects can be neglected, that is, when surface areas and pore size distributions are equivalent for the MIP and corresponding NIP. Additionally, the silica surface can be further utilized for template immobilization in surface and hierarchical imprinting strategies. Further work is being carried out

Table II. Retention Times of Ephedrine Enantiomers on the MIP and on the NIP Packed Columns

	Retention time, t_r (min)	
	MIP	NIP
(+)-Ephedrine	2.41	1.80
(−)-Ephedrine	2.86	1.79
$NaNO_2$ (Void)	1.87	1.68

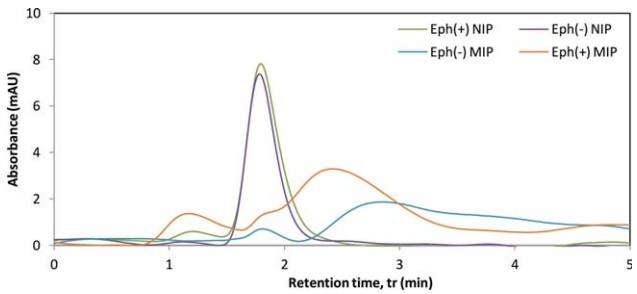

Figure 4. Overlay of chromatography profiles of the template (−)-ephedrine and the enantiomer (+)-ephedrine on the NIP and the MIP columns. 95% MeOH/5% 100 m*M* NH_4Ac (pH 3.6), 1 mL/min. [Color figure can be viewed in the online issue, which is available at wileyonlinelibrary.com.]

to explore this approach and its potential benefits for the creation of improved molecular imprints in crosslinked polymers, utilizing other formats of inorganic templates such as porous silica particles and surface modified silica nanoparticles.

ACKNOWLEDGMENTS

The authors acknowledge the financial support by the European Commission, under the 7th Framework programme, integrated in the PepMIP project: "Robust affinity materials for applications in proteomics and diagnostics," grant # 264699.

REFERENCES

1. Wackerlig, J.; Schirhagl, R. *Anal. Chem.* **2015**, *88*, 250.
2. Tokonami, S.; Shiigi, H.; Nagaoka, T. *Anal. Chim. Acta* **2009**, *641*, 7.
3. Gutiérrez-Climente, R.; Gómez-Caballero, A.; Halhalli, M.; Sellergren, B.; Goicolea, M. A.; Barrio, R. J. *J. Mol. Recognit.* **2016**, *29*, 106.
4. Vasapollo, G.; Sole, R. D.; Mergola, L.; Lazzoi, M. R.; Scardino, A.; Scorrano, S.; Mele, G. *Int. J. Mol. Sci.* **2011**, *12*, 5908.
5. Haginaka, J. *J. Chromatogr. B* **2008**, *866*, 3.
6. Oxelbark, J.; Legido-Quigley, C.; Aureliano, C. S. A.; Titirici, M.; Schillinger, E.; Sellergren, B.; Courtois, J.; Irgum, K.; Dambies, L.; Cormack, P.; Sherrington, D.; De Lorenzi, E. *J. Chromatogr. A* **2007**, *1160*, 21.
7. Tamayo, F. G.; Titirici, M.; Martin-Esteban, A.; Sellergren, B. *Anal. Chim. Acta* **2005**, *542*, 38.
8. Titirici, M.; Hall, A. J.; Sellergren, B. *Chem. Mater.* **2002**, *14*, 21.
9. Yilmaz, E.; Ramstrom, O.; Moller, P.; Sanchez, D.; Mosbach, K. *J. Mater. Chem.* **2002**, *12*, 1577.
10. Zhou, T.; Jorgensen, L.; Mattebjerg, M. A.; Chronakis, I. S.; Ye, L. *RSC Adv.* **2014**, *4*, 30292.
11. Zhou, T.; Zhang, K.; Kamra, T.; Bulow, L.; Ye, L. *J. Mater. Chem. B* **2015**, *3*, 1254.
12. Mohamed, M. H.; Wilson, L. D. *Nanomaterials* **2012**, *2*, 163.
13. Yan, H.; Row, K. *Int. J. Mol. Sci.* **2006**, *7*, 155.
14. Xie, S.; Svec, F.; Fréchet, J. M. J. *Chem. Mater.* **1998**, *10*, 4072.
15. Nicholls, I. A.; Andersson, H. S.; Golker, K.; Henschel, H.; Karlsson, B. C. G.; Olsson, G. D.; Rosengren, A. M.; Shoravi, S.; Suriyanarayanan, S.; Wiklander, J. G.; Wikman, S. *Anal. Bioanal. Chem.* **2011**, *400*, 1771.
16. Wei, S.; Jakusch, M.; Mizaikoff, B. *Anal. Bioanal. Chem.* **2007**, *389*, 423.
17. Ramström, O.; Ansell, R. J. *Chirality* **1998**, *10*, 195.
18. Duarte, M.; Billing, J.; Liu, Y.; Leeman, M.; Karlsson, O. J.; Yilmaz, E. *Macromolecules* **2015**, *48*, 4382.
19. Piletsky, S. A.; Karim, K.; Piletska, E. V.; Day, C. J.; Freebairn, K. W.; Legge, C.; Turner, A. P. F. *Analyst* **2001**, *126*, 1826.
20. Ansell, R. J.; Kuah, J. K. L.; Wang, D.; Jackson, C. E.; Bartle, K. D.; Clifford, A. A. *J. Chromatogr. A* **2012**, *1264*, 117.
21. Ramstrom, O.; Yu, C.; Mosbach, K. *J. Mol. Recognit.* **1996**, *9*, 691.
22. Dong, X.; Sun, H.; Lu, X.; Wang, H.; Liua, S.; Wang, N. *Analyst* **2002**, *127*, 1427.
23. Maier, N. M.; Lindner, W. *Anal. Bioanal. Chem.* **2007**, *389*, 377.
24. Brunauer, S.; Emmett, P. H.; Teller, E. *J. Am. Chem. Soc.* **1938**, *60*, 309.
25. Mosbach, K.; Ramstrom, O. *Nat. Biotechnol.* **1996**, *14*, 163.
26. Ansell, R. J.; Kuah, K. L. *Analyst* **2005**, *130*, 179.
27. Piletsky, S. A.; Mijangos, I.; Guerreiro, A.; Piletska, E. V.; Chianella, I.; Karim, K.; Turner, A. P. F. *Macromolecules* **2005**, *38*, 1410.
28. Ansell, R. J.; Wang, D. *Analyst* **2009**, *134*, 564.
29. Deng, D. L.; Zhang, J. Y.; Chen, C.; Hou, X. L.; Su, Y. Y.; Wu, L. *J. Chromatogr. A* **2012**, *1219*, 195.
30. Brisbane, C.; McCluskey, A.; Bowyer, M.; Holdsworth, C. I. *Org. Biomol. Chem.* **2013**, *11*, 2872.